Mater. Res. Soc. Symp. Proc. Vol. 903E © 2006 Materials Research Society 0903-Z06-05.1

Grain Boundary Structure Evolution in Nanocrystalline Al by Nanoindentation Simulations

V. Dupont and F. Sansoz
School of Engineering, The University of Vermont, Burlington, VT 05405 USA

ABSTRACT

The nanoindentation of a columnar grain boundary (GB) network in nanocrystalline Al has been examined by atomistic simulation. The goal of this study was to gain fundamental understanding on the relationship between structure evolution at GBs and incipient plasticity for indenter tips significantly larger than the average grain size. The nanoindentation simulations were performed by quasicontinuum method at zero temperature. A GB network made of vicinal and high-angle <110> tilt GBs was produced by generating randomly-oriented 5-nm grains at the surface of a 200 nm-thick film of Al. The major findings of this investigation are that (1) nanocrystalline GB networks profoundly impact on the nanoindentation response and cause significant softening effects at the tip/surface interface; (2) GB movement and deformation twins are found to be the predominant deformation modes in columnar Al, in association with shear band formation by GB sliding and intragranular slip, and crystal growth by grain rotation and coalescence; and (3) the cooperative processes during plastic deformation are dictated by the atomic-level redistribution of principal shear stresses in the material.

INTRODUCTION

It has been recently demonstrated that grain boundary (GB) structures have a profound impact on the deformation of nanocrystalline metals. For example, Sansoz and Molinari [1] have predicted by atomistic simulation that the GB behavior of sliding and migration, which are key deformation mechanisms at small grain size, can be controlled by tailoring the GB structural units. Moreover, new evidence of grain growth via GB movement mechanisms has been found in nanocrystalline Al at room temperature under *in-situ* TEM nanoindentation [2]. Similarly, recent observations of rapid-grain growth at room and cryogenic temperatures have been obtained in nanocrystalline Cu under micro-indentation [3]. However, this atypical behavior of GB structure evolution under indentation is not fully understood at present time.

This study intends to provide new insights on the evolution of GB networks in nanocrystalline Al films deformed by nanoindentation using atomistic modeling. Earlier atomistic studies [4-6] have already addressed the nanoindentation of 3D nanocrystalline metal films at zero and finite temperatures. Van Swygenhoven and co-workers [4] have predicted on nanocrystalline Au that GBs can act as source and sink for dislocations nucleated at the indenter-substrate contact, which caused some softening effects as compared to single crystal films. These authors have found that GB sliding and grain rotation occur at very small grain size at finite temperature, but these mechanisms were less easily observed at zero temperature. Other authors [5,6] have also predicted that the elastic limit of thin films can be significantly decreased when indentation occurs on or near GBs. No atomistic studies, however, have shown the occurrence of grain growth under nanoindentation at low temperature. The fact that the above atomistic studies considered friction-less spherical indenters with a curvature radius smaller than

the average grain size may support the assumption that modeling larger indenters is necessary in atomistic simulation. This aspect is particularly important since the experimental nanoindentation techniques such as the atomic force microscope or nanohardness tester, have tip radius significantly larger than the average grain size of nanocrystalline metals [7].

This study presents the results of quasi-2D atomistic simulations of 200 nm-thick films of Al indented by a 15 nm-radius tip. Both single crystal and 5 nm-grain size thin films were investigated. The simulations were performed at zero temperature using the quasicontinuum method. The next section will provide the details of the simulation method. We discuss in the last section the effects of GB structure network on the underlying deformation mechanisms, and show that the redistribution of stress gradients across grains plays a central role on these effects.

SIMULATION METHOD

Both film and indenter geometries were simulated using the quasicontinuum method [8]. This technique provides the solution of equilibrium atomic configurations by energy minimization, given externally imposed forces or displacements; and does not explicitly represent every atom in the simulation cell. In fact, the regions of small deformation gradients are treated as continuum zones by finite element method. The present model is schematically given in Fig. 1.a. The indenter was represented by an aluminum cylinder with a radius of 15 nm. The film dimensions were 400nm × 200nm × 0.286nm. A periodic boundary condition was imposed in the out-of-plane direction. The size of the atomistic zone was 50nm × 25nm. The atomic structure of the different zones was defined as follows. The indenter was considered single crystalline with the orientation provided in Fig. 1a. Two structures were studied for the film. The first structure consisted in a single crystal with a (111) surface and a $[1\bar{1}0]$ out-of-plane direction. The second structure investigated, a polycrystal, was constructed as follows. Reference atoms were placed randomly in the sample at an average distance equal to the average grain size and GBs were formed by a Voronoi construction which was based on a constrained-Delaunay connectivity scheme. For this study, the average grain size was 5 nm.

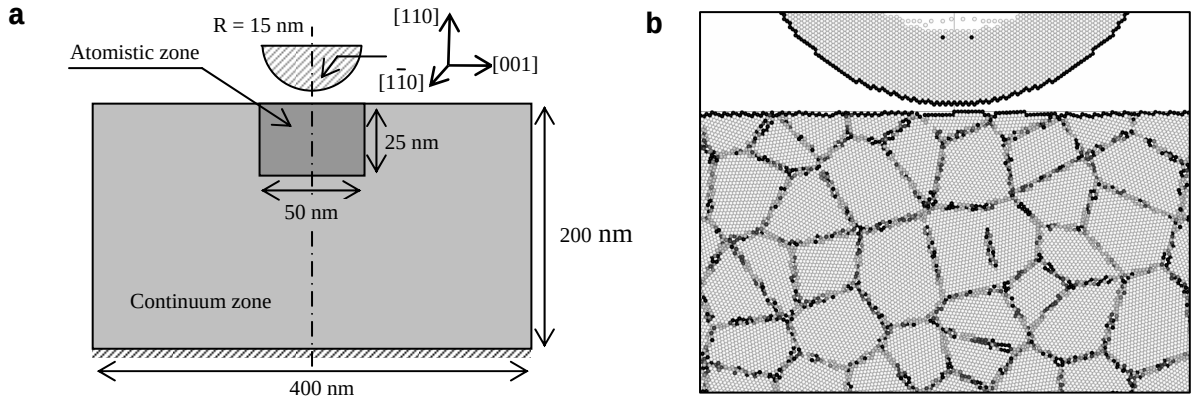

Figure 1. (a) Schematic representation of the continuum and fully-atomistic zones simulating the nanoindentation of 200nm-thick Al films. (b) Partial view of the fully-atomistic zone showing the GB network after zero force energy minimization of randomly-oriented columnar $[1\bar{1}0]$ tilt grains. The average grain size under the indenter is about 5 nm.

Each grain was assigned a common tilt axis along $[1\bar{1}0]$ and random in-plane orientation. Starting from the reference atom, the other atoms of the grains were added according to the Bravais lattice cell [9]. We fixed the orientation of the first grain of the film in contact with the indenter to match that of the single crystal model. Furthermore, in order to avoid the discontinuities in the energy state at the continuum/atomistic frontier, the latter was modelled using a single crystal with the orientation of the single crystal model described above. A total number of 50 grains were fully represented in the atomistic zone under the indenter. We used an embedded-atom- method (EAM) potential for Al by Voter and Chen [10]. The energy minimization was performed at zero temperature by conjugate gradient method. The sample was first relaxed under zero force lattice static conditions in order to obtain the lowest state of energy. The indenter was kept completely rigid and we fixed the bottom of the film. A partial view of the resulting nanostructure after relaxation is shown in Fig. 1b. After this step, the atoms of the indenter were displaced by increment of 0.75Å until the depth of penetration reached 7.5 nm. Energy minimization was performed between each loading steps.

In order to detect the presence of planar defects and GB structure evolution with respect to the elastically deformed crystal domain, the centrosymmetry parameter proposed by Kelchner et al. [11] was used. Our coloring scheme for this parameter is as follows. Atoms in perfect fcc sequence are colored in white, those with a hcp structure or representing a stacking fault are colored in light grey, and those with low crystal symmetry are clored in dark grey. The force on the indenter was calculated by adding the out-of-balance forces obtained on each indenter atom and projected along the direction of indentation. The local stress tensor of the i^{th} atom, $\tilde{\sigma}_i$,was calculated in the full atomistic region using the formula provided by Lilleodden et al. [6], which can be simplified as follows:

$$\sigma_i^{\alpha\beta} = \frac{1}{\omega_i^0 \, Det[F_i^{\alpha\beta}]} \left\{ \frac{1}{2} \sum_j \left(-\frac{1}{r} \frac{\partial \varphi}{\partial r} \right) r^\alpha r^\beta \Big|_{r=r_{ij}} \right\} \tag{1}$$

where α and β are the Cartesian coordinates, ω_i^0 is the undeformed atomic volume of the i^{th} atom, $Det[F_i^{\alpha\beta}]$ is the determinant of the deformation gradient, φ is the interatomic potential, and r_{ij} is the distance between i^{th} and j^{th} atoms. Note that the kinetics terms have been eliminated in equation (1) as compared to ref. [6]. In this equation, the use of the determinant of the deformation gradient has been shown to provide improved accuracy for the calculation of deformed atomic volumes. Furthermore, the principal shear stress, τ, was calculated for each atom using the components of the atomic-level stress tensor $\tilde{\sigma}_i$ using the formula in ref. [12].

RESULTS AND DISCUSSION

Single crystal deformation

Our simulation of indentation of the single crystal film was found to be in good agreement with the results of the literature. It was observed for example that the onset of plasticity in the film occurs by nucleation of <112> dislocations emanating from the tip/surface interface. Our model also accurately predicted the effects of adhesion and interfacial friction at the early stage of indentation. These effects were found to displace the maximum value of principal shear stress closer to the tip/surface interface, in accordance with the elastic theory [12].

Grain boundary deformation mechanisms

The deformation mechanisms of nanoindentation strongly vary in the presence of GB networks as shown in Fig. 2. A large number of <112> partial dislocations and deformation twins, which were often nucleated in grains that are not directly in contact with the indenter, can be observed in Fig. 2a. Consistent to the existing literature, the GB structure dominates the dislocation nucleation process and also serves as dislocation sink. Additionally, we found that the partial dislocations nucleated preferentially from triple-junctions in order to accommodate GB sliding. GB sliding occurs at early stage due to atom shuffling. This mechanism is well-known and has been detailed elsewhere [1,4]. Our simulation also shows that GB sliding is associated with significant grain rotation and results in the formation of thin shear bands. Figures 2b and 2c illustrate our simulation of the first shear band by grain rotation. It is worth noting in Fig. 2c that the extension of the shear band in grain 2 was made possible by intragranular slip in the prolongation of the interface between grains 3 and 4. Furthermore, a twin was grown in grain 2 from parallel partial dislocations emitted by the same interface. For larger depths of indentation, significant GB movement was observed and, to some extent, linked to the twin growth process. GB movement in association with grain rotation caused cooperative grain behaviors as shown in Fig. 2d. In this example, it is possible to observe simultaneous events of grain coalescence (grains 2 and 3), disappearance (grain 1) and growth (grains 4 and 5).

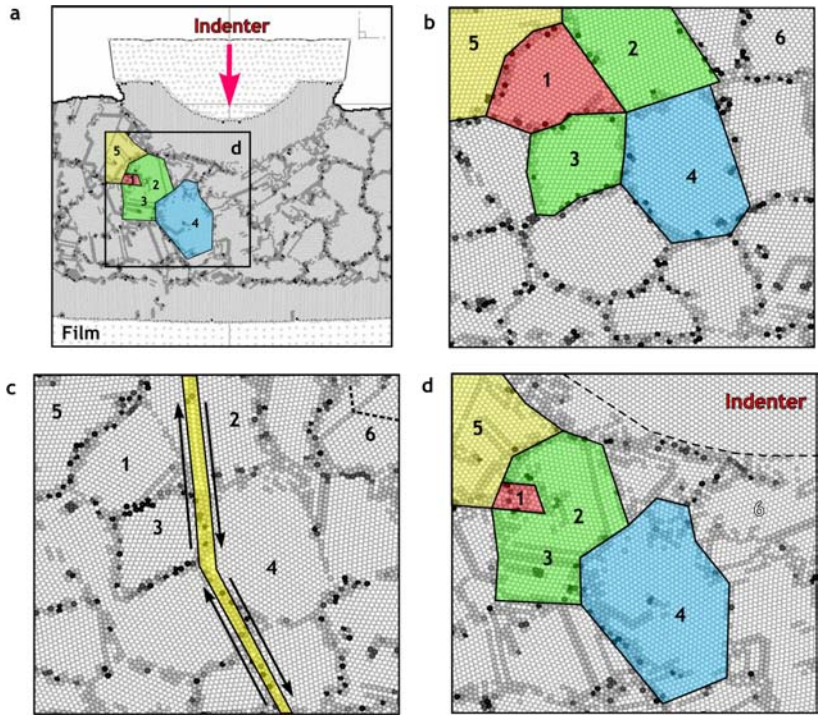

Figure 2. (a) Grain boundary network after indentation. Grains 1-5 have been colored for reference. Different stages of deformation in the shaded area shown in (a) are given as follows: (b) after initial relaxation and before indentation; (c) at 2.5 nm-indentation depth coinciding with the formation of the first shear band; and (d) at 7.5 nm-indentation depth, disappearance of grain 1 in association with the coalescence of grains 2 and 3. Significant grain growth can be observed in grains 4 and 5. A deformation twin (dashed line) can also be seen migrating in grain 6.

Stress analysis

In Fig. 3a, we have plotted the normalized contact area as a function of the normalized force, for both polycrystal and single crystal Al, and the elastic contact theory of Johnson, Kendall and Roberts [12]. This figure shows that the simulation deviates from the elastic theory at a specific applied load, which corresponds to the onset of plasticity in the film. It can be concluded that the polycrystal yields plastically at lower applied force than the single crystal. Therefore, strong softening effects exist when nanocrystalline GBs are indented. We assume that this behavior is related to the GB sliding process described above at early indentation stage.

In order to gain additional insights on the role played by the stress on the deformation mechanisms, we have examined the evolution of principal shear stress obtained at atomic-level for different steps of indentation. Figure 3b shows the distribution of principal shear stresses before indentation. We can clearly see in this figure that shear stresses are higher in the GB area as compared to the grain interior. This observation seems to explain why dislocations were found to nucleate preferentially on GB sites. Figure 3c represents the principal shear stresses at the loading step preceding the first shear band formation. It can be seen in this figure that the stress is higher in the region of intragranular slip in grain 2. More importantly, our simulation clearly shows that grain rotation causes significant decrease of the gradient of principal shear stress across the interfaces. In Fig. 3d corresponding to the maximum applied load, it is even difficult to relate the stress pattern to the grain structure because of the significant redistribution of principal shear stresses.

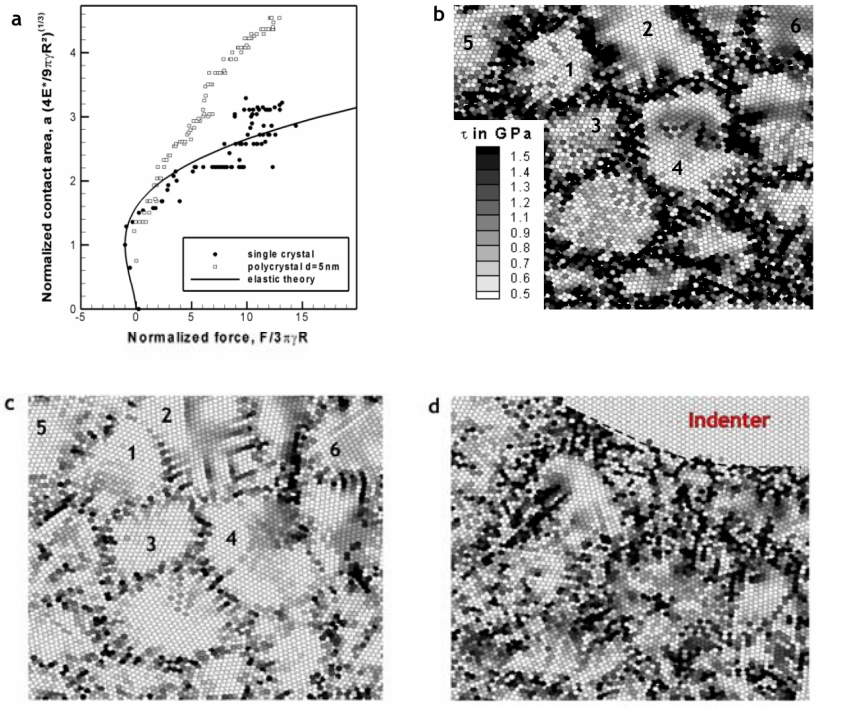

Figure 3. (a) Evolution of the normalized contact area as a function of the normalized force for single crystal film (plain circles), 5nm-grain size film (open circles) and the Johnson-Kendall-Roberts (JKR) model (line). (b)-(d) Atomic-level distribution of principal shear stress τ at different stages of indentation.

Cooperative processes during plastic deformation of nanocrystalline metals have already been predicted in pure compression by molecular dynamics at 800K [13]. In the present study, however, we found similar mechanisms for the first time at 0K under nanoindentation of nanocrystalline Al. We can interpret this result in nanocrystalline Al by the fact that under nanoindentation, large plastic strain can be reached without intense intragranular dislocation activity. This mechanism is somewhat reminiscent from recent reports of continuous dynamic recrystallization in superplasticity of Al-alloys [14]. The latter process is defined by the homogeneous evolution of the grain structure that involves the migration of high-angle GB. This suggests that further efforts should be directed toward understanding the relationship between GB structural units in nanocrystalline Al and GB movement.

CONCLUSIONS

This study shows for the first time the simulation of growth, disappearance and coalescence of nanosized grains under nanoindentation at zero temperature. Our conclusions can be drawn as follows: (1) nanocrystalline GB networks profoundly impact on the nanoindentation response and cause significant softening effects at the tip/surface interface; (2) GB movement and deformation twins are found to be the predominant deformation modes in columnar Al, in association with shear band formation by GB sliding and intragranular slip, as well as crystal growth by grain rotation and coalescence; and (3) the cooperative grain behavior is dictated by the atomic-level redistribution of principal shear stresses at the grain interfaces.

ACKNOWLEDGEMENTS

The author would like to acknowledge support from the Vermont Experimental Program to Stimulate Competitive Research (VT EPSCoR) under grant number NSF EPS 0236976.

REFERENCES

1. F. Sansoz and J. F. Molinari, *Acta Mater* **53**, 1931 (2005).
2. M. Jin, A. M. Minor, E. A. Stach and J. W. Morris Jr., *Acta Mater* **52**, 5381 (2004).
3. K. Zhang, J. R. Weertman and J. A. Eastman, *Appl. Phys Lett.* **87**, 061921 (2005).
4. D. Feichtinger, P. M. Derlet and H. Van Swygenhoven, *Phys Rev B* **67**, 024113 (2003).
5. X. L. Ma and W. Yang, *Nanotechnology* **14**, 1208 (2003).
6. E. T. Lilleodden, J. Zimmerman, S. M. Foiles and W. D. Nix, *J. Mech. Phys. Solids* **51**, 901 (2003).
7. J. Chen, W. Wang, L. H. Qian and K. Lu, *Scripta Mater* **49**, 645 (2003).
8. R. Miller, E. B. Tadmor, *J. Comput. Aided Mater. Des.* **9**, 203 (2002).
9. A. Brokman and R. W. Balluffi, Acta Metall. **29**, 1703 (1981).
10. A. F. Voter and S. P. Chen, Mat. Res. Soc. Symp. Proc. **82**, 175 (1987).
11. C. L. Kelchner, S. J. Plimpton and J. C. Hamilton, *Phys Rev B* **58**, 11085 (1998).
12. K. L. Johnson, K. Kendall and A. D. Roberts, *Proc R Soc London A* **324**, 301 (1971).
13. A. Hasnaoui, H. Van Swygenhoven and P. M. Derlet, *Phys. Rev. B* **66**, 184112 (2002).
14. L. M. Dougherty, I. M. Roberston, J. S. Vetrano, *Acta Mater* **51**, 4367 (2003).